

Document downloaded from:

<http://hdl.handle.net/10251/200297>

This paper must be cited as:

Favero, D.; Marcon, V.; Agnol, LD.; Gómez, CM.; Cros, A.; Garro, N.; Sanchis Sánchez, MJ.... (2022). Effect of chain extenders on the hydrolytic degradation of soybean polyurethane. *Journal of Applied Polymer Science*. 139(28):1-13.
<https://doi.org/10.1002/app.52623>



The final publication is available at

<https://doi.org/10.1002/app.52623>

Copyright John Wiley & Sons

Additional Information

EFFECT OF CHAIN EXTENDERS ON THE HYDROLYTIC DEGRADATION OF SOYBEAN POLYURETHANE

Diana Favero¹, Victória Marcon¹, Lucas Dall Agnol¹, Clara M. Gómez², Ana Cros², Nuria Garro², Maria J. Sanchis³, Marta Carsí⁴, Carlos A. Figueroa¹, Otávio Bianchi^{1,5*}

¹ *Postgraduate Program in Materials Science and Engineering (PGMAT), University of Caxias do Sul (UCS), Caxias do Sul, RS, Brazil;*

² *Instituto de Ciencia de los Materiales, Universidad de Valencia, 46980 Paterna, València, Spain;*

³ *Department of Applied Thermodynamics, Institute of Electric Technology, Universitat Politècnica de València, Spain;*

⁴ *Department of Applied Thermodynamics, Instituto de Automática e Informática Industrial, Universitat Politècnica de Valencia, 46022 Valencia, Spain;*

⁵ *Department of Materials Engineering (DEMAT), Federal University of Rio Grande do Sul (UFRGS), Porto Alegre, RS, Brazil.*

***Corresponding author.** Tel: +55 (54) 984030958; E-mail address: otavio.bianchi@gmail.com (Bianchi O.)

ABSTRACT

This publication highlights the effect that different chain extenders (CEs) have on the structure-property relationships of soy-based polyurethanes that have been exposed to hydrolytic degradation for 480 and 960 h at 80°C. Gel content, crosslinking densities, surface energy, atomic force microscopy, dielectric and dynamic mechanics were used for monitored structural changes. When a chain extender is not used, PU is composed of a structure with less phase separation, maintaining all properties over time. However, when a chain extender, butane-1,4-diol (BDO), ethane-1,2-diol (MEG) or (2-hydroxypropoxy)-propane-2-ol (DPG) are added, it is noted that there is a more significant degradation in the flexible domains, modifying the fraction between the initial rigid(HS)/soft (SS) segment that makes the polymer stiff and brittle. The hydrolysis degradation generates new FTIR bands relative to urea (1640 cm⁻¹) and amide (1800 cm⁻¹). The reduction in band intensity of the C=O_{free} at 1730 cm⁻¹, while increasing the intensity of C=O_{bonded} at 1710 cm⁻¹ indicated a higher phase separation degree. After 960 h the T_{gS} decreased, while the T_{gH} was practically unchanged. The higher polarization observed in the PUs with BDO and MEG samples is a good indicator of the increased phase separation resulting in hydrolytic degradation.

Keywords: soybean oil polyol; soybean polyurethane; chain extender; hydrolytic degradation; dielectric relaxation spectroscopy.

1. INTRODUCTION

Soy polyurethanes (SPUs) are biocompatible, have good availability and are inexpensive [1]. The SPUs are produced from the soybean oil polyol (SOP), a natural, biodegradable and non-toxic renewable source. The main SPUs applications are in the area of coatings [1] and thermal insulation [2], and some of these materials are in the commercialization process. However, when in contact with water, acids, and alkalis, these materials undergo backbone degradation. This alters its structure and, consequently, deteriorates its physical-mechanical properties, which directly reflect the valuable life reduction of these materials. For example, in applications where these materials are subjected to hydrolysis reactions, such as in contact with water and others, hydrolytic stability is crucial and serves as an indicator of durability in use [3]. Therefore, it is essential to understand the hydrolysis mechanisms, as they help choose the application and predict long-term durability and resistance [3, 4].

SPUs can be very promising in the plastic industry and still are new applications to be used shortly. Modifying their formulations allow to obtain a broad spectrum of tailor-made properties, as a function of the hard and soft segments employed. SOP forms the soft segment (SS), responsible for the rubber-like characteristics and elastomer elasticity. The hard segment (HS) is formed by reaction of isocyanate ($-NCO$) with short-chain diols used as chain extenders (CEs) that affect mechanical characteristics such as hardness, elasticity, and tear strength [5]. Thus, SPUs depicts high resistance advantage to hydrolysis and a low degradation rate at low temperatures compared to other polyurethanes (PUs). As expected, the hydrolytic degradation of PUs from polyethers from vegetable oils occurs at a much slower rate than polyester, with similar behavior to PUs with polyols from petrochemical sources. This is due to the ether group stability in aqueous media [6]. However, the hydrolytic degradation mechanism is very similar [7]. This mechanism happens primarily in the amorphous region (soft domain) when the PU comes into contact with water, through the hydrolysis reaction that generates carboxylic ester groups cleavage resulting in the formation of alcohol ($-OH$) and a carboxylic acid ($-COOH$) [3, 8, 9]. Secondly, in the organized domain, (hard) the urethane group generates alcohol and an amine [3, 10, 11]. The amine specie formed is directly related to the kind of isocyanate used either aliphatic or aromatic [6]. The ester can hydrolyze bonds by about an order of magnitude faster than urethane bonds, making many polyesters easily degradable or biodegradable [11]. When comparing polyester PUs, the carboxylic acid (generated in the first step) makes the hydrolysis reaction autocatalytic [8, 11], while in polyether PUs, the hydrolysis reaction tends to occur initially in the urethane group. In both chain scission steps, it is evident that cleavage of the urethane group reduces the mechanical properties [12].

From a general point of view, the nature of the flexible and rigid segments plays a fundamental role in the hydrolytic stability of PUs [13, 14]. Due to their hydrophobic character, many polyols from

renewable sources can repel water [15-17]. However, as a rule, the formation of organized structures can decrease the rate of hydrolytic degradation due to less water diffusion [3, 4]. For example, the hydrolytic stability of castor oil PUs with propylene glycol (PPG) as a chain extender in water (70 °C), ethanol, and saline for 60 days resulted in a reduction in molecular weight mainly due to low crosslink density. This effect was attributed to the hydrophilic character of PPG, which makes it more susceptible to bond cleavage and water absorption [18]. Nevertheless, depending on the vulnerability of the urethane bond to water, the resistance to hydrolytic degradation can be altered[19].

PUs based on renewable sources have gained prominence in scientific and industrial research [17]. Nonetheless, the effect of hydrolytic degradation on the structure and properties of these materials is still little explored. Other crucial points are that using physicochemical approaches, spectroscopic techniques, dielectric relaxation spectroscopy (DRS), dynamic mechanical analysis (DMA) combined with microscopic techniques can provide a valuable tool to investigate effects associated with hydrolytic degradation and its impact on relaxations and molecular structure. Thus, information about the state of the backbone chain and how it is affected by degradation becomes crucial for a better choice of monomers for a specific PUs application [5, 8, 11, 18, 20].

This article's main objective was to evaluate the effect of time on hydrolytic degradation in polyether SPUs with different ECs in an aqueous medium at 80 °C for up to 960 h. It is expected that, as SOP is a polyester/polyether based microdiol, the physical-mechanical properties will be less affected in relation to the deterioration of its properties over time. In this way, we hope to understand better the effect that hydrolytic degradation has on SPUs to predict future applications.

2. EXPERIMENTAL

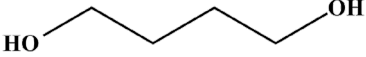
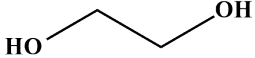
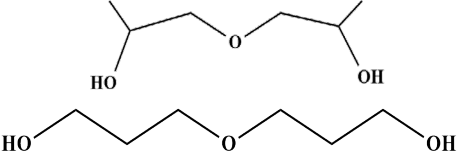
2.1. Materials

The soybean oil polyol (SOP) was obtained with molecular weight 1463 g.mol^{-1} , hydroxyl number $190 \text{ mg.KOH.g}^{-1}$ and glass transition temperature $\sim -80^\circ\text{C}$ according to D. Favero et al. [5, 21]. 4,4'-diphenylmethane-diisocyanate (MDI; CAS number 101-68-8) with $33.49 \pm 0.07 \text{ wt.}\%$ free isocyanate index and 2.0 functionality was supplied by BASF (MDI). Different CEs as butane-1,4-diol (BDO); CAS number 110-63-4) was purchased from BASF, ethane-1,2-diol (MEG); CAS number 107-21-1) was purchased from Sigma-Aldrich and (2-hydroxypropoxy)propan-2-ol (DPG); CAS number 2526-71-8) was purchased from Down Brazil, these raw materials were used. The chain extenders were distilled before use. These raw materials were used for the PU films synthesis ($\sim 500 \mu\text{m}$ thickness).

2.2. Synthesis of SPU with different CEs

SPUs with different CEs were obtained by one-step bulk polymerization, without any catalyst, with approximately hard segment 39 wt.% and 1.1/1.0 OH/NCO molar ratio. The MDI was heated at 45 °C for 5 min. Then, the polyol, MDI, and CE were mixed for approximately 40 s stirred slowly to prevent bubbles formation. To evaluate the CEs effect, a sample was prepared without CE; SOP/MDI material denoted as: PU-PURE. The polyurethanes obtained as a function of chain extender have been designated as PU-CE. Details on the synthesis and preparation of SPUs have been described previously [5]. Table 1 compiles the different chain extender and soy polyurethanes studied in this paper.

Table 1. Description of chain extenders (CE) and soy polyurethanes (SPU)

CE IUPAC name (abbreviation)	Molar weight (g.mol ⁻¹)	structural formula CE	SPU
butane-1.4-diol (BDO)	90.12		PU-BDO
ethane-1.2-diol (MEG)	62.06		PU-MEG
(2-hydroxypropoxy)- propane-2-ol (DPG)	134.17		PU-DPG

2.3. Hydrolytic degradation of SPUs

Before characterizing hydrolytic degradation, SPUs were oven-dried at 80 °C for 24 hours. Then, SPUs were fully immersed in distilled water for 480 h and 960 h at 80 °C according to the ASTM- D3137 standard procedure.

CHARACTERIZATION TECHNIQUES

ATR-FTIR monitored the functional groups formed during the hydrolysis experiments. This was performed using the Perkin-Elmer Spectrum 400 Spectrometer equipment in attenuated total reflection (diamond crystal at 45°) mode. The spectra were obtained by averaging 32 scans in the 4000–450 cm⁻¹ region with a 2 cm⁻¹ resolution.

The crosslink density of SPU before and after hydrolysis experiments was determined from the swelling degree. The films were initially dried at 80 °C for 24 h; subsequently, they were immersed in xylene solvent (8.88 cal.cm⁻³ solubility parameter, 123.31 cm³.mol⁻¹ molar volume, and 0.861 g.cm⁻³ density) until reaching the equilibrium (thirty days). The swelling degree was determined through Eq. 1 [22]:

$$Q = \frac{m_i - m_0}{m_0} \cdot \frac{\rho_P}{\rho_s} \quad (1)$$

wher, Q is the swelling coefficient, m_i is the swollen polymer mass at equilibrium (g), m_0 is the polymer mass before swelling (g), ρ_P is the polymer density (g.cm⁻³), and ρ_s is the solvent density (g.cm⁻³). Thus, the crosslinking density (ν) for all SPUs was determined by Eq. 2 [23]:

$$\nu = \frac{-[V_r + \chi V_r^2 + \ln \ln (1 - V_r)]}{\rho_r V_0 \left(V_r^{1/3} - \frac{V_r}{2} \right)} \quad (2)$$

where, $V_r = \frac{1}{1+Q}$ is the polymer volume fraction in the swelled polymer, χ is the polymer-solvent interaction parameter (normally, the χ value is 0.34) [20]. V_0 is the solvent molar volume and ρ_r is the polymer density.

The surface free energy of the materials was determined by contact angle measurements with standard liquids. The measurements were carried out in an SEO® Phoenix100 (Korea) instrument and four probe liquids were employed at 23 °C: dimethyl formamide ($\gamma_L^P = 4.88$ mJ/m²; $\gamma_L^D = 32.42$ mJ/m²; $\gamma_L = 37.3$ mJ/m²), glycerin ($\gamma_L^P = 29.7$ mJ/m²; $\gamma_L^D = 33.6$ mJ/m²; $\gamma_L = 63.3$ mJ/m²), distilled water ($\gamma_L^P = 51.0$ mJ/m²; $\gamma_L^D = 21.8$ mJ/m²; $\gamma_L = 72.8$ mJ/m²) and n-hexadecane ($\gamma_L^P = 0.0$ mJ/m²; $\gamma_L^D = 27.6$ mJ/m²; $\gamma_L = 27.6$ mJ/m²); where: γ_L^P , γ_L^D and γ_L represent the polar component, the dispersive component and the liquids surface free energy, respectively [24, 25]. The sessile drop method was adopted using 2 μ L drops. The contact angle was measured at least ten times at different sites on the surface for the average value consideration.

The surface morphology of the SPUs before and after hydrolysis was evaluated by atomic force microscopy (AFM, Nanotec). The AFM was performed in dynamic tapping mode (23°C). The amplitude set point was adjusted at 65% of the free amplitude value to set the tip-sample interaction in the moderate force range. At least five different regions of the surface of the samples were digitized to attest to the results' reproducibility.

The solid linear viscoelastic behavior of SPUs was performed by DMA analysis (TA Instruments, 2890 model) using tensile film clamp in the range of temperature from -125 °C to 179 °C (1 Hz, 20 μm, and a heating rate at 3 °C.min⁻¹). Samples with 15.0 mm length × 6.0 mm width × 0.5 mm dimensions were used. All experiments were performed in triplicate.

DRS measurements in the frequency range from 5×10^{-2} to 3×10^6 Hz were performed using a Novocontrol Broadband Dielectric Spectrometer (Hundsagen, Germany) consisting of an Alpha analyzer. The measurements were performed in N₂ atmosphere from 140 °C to 160 °C in steps of 5 °C using the temperature control system of a Novocontrol Quatro cryosystem, with an accuracy of ± 0.1 °C during each sweep in frequency. Samples with disc-shaped about 0.1 mm thickness and 40 mm diameter were used. To avoid the conductivity increase due to water, before these measurements, the samples were placed at 50 °C on a stove for 24 hours until a constant weight was reached. The experimental uncertainty was better than 5% in all cases.

RESULTS AND DISCUSSION

The hydrolytic degradation in SPUs can be monitored by the formation of new chemicals or by reducing band intensity. The changes in the SS and HS characteristic bands due to the hydrolytic degradation at different times (480 h and 960 h) can be detected in the FTIR spectra of PU-PURE, PU-DPG, PU-MEG, and PU-BDO (Fig. 1a-d). All the dry PUs named as 0 h (without hydrolytic degradation) are also presented as a comparison effect in these spectra. All SPUs show two overlapping bands on the carbonyl stretching region (C=O), one dominant peak centered at 1730 cm⁻¹ and a broad shoulder close to 1710 cm⁻¹. These bands are ascribed to the stretching vibrations of free carbonyl (C=O_{free}) (non-hydrogen-bonded) and bonded carbonyl (C=O_{bonded}), respectively [5]. The gradual change in signal strength due to degradation shows that the original hydrogen bonds are no longer the same. This is because new chemical groups are formed like acid, amine, and others [26-28]. Since most of the C=O_{free} group's are ascribed to the soft segments, there was a decreased tendency of these vibrations due to ester and urethane (H₂N-CO-R) groups chain scission [13]. While the C=O_{bonded} vibration increased the intensity, there were changes in the phase separation degree between the soft and hard segments [26, 29]. In these spectra, it was also evidenced the urea group intensity increased at 1640 cm⁻¹. After being immersed in water, this is the reaction product between the isocyanate and the amine group. This secondary reaction leads to a decrease in PUs molecular weight [30]. The δN-H + νC-N intensity increases at 1511 cm⁻¹ indicated the HS hydrolytic degradation [28]. Besides, in these spectra appears one new absorption band at 1800 cm⁻¹ called amide I carbonyls stretching vibrations characteristic [28]. When immersed in water, this is the reaction

product between the isocyanate and the carboxylic acid [13]. The C–C vibration band at 1412 cm^{-1} was used as the standard for relative comparison between the PUs.

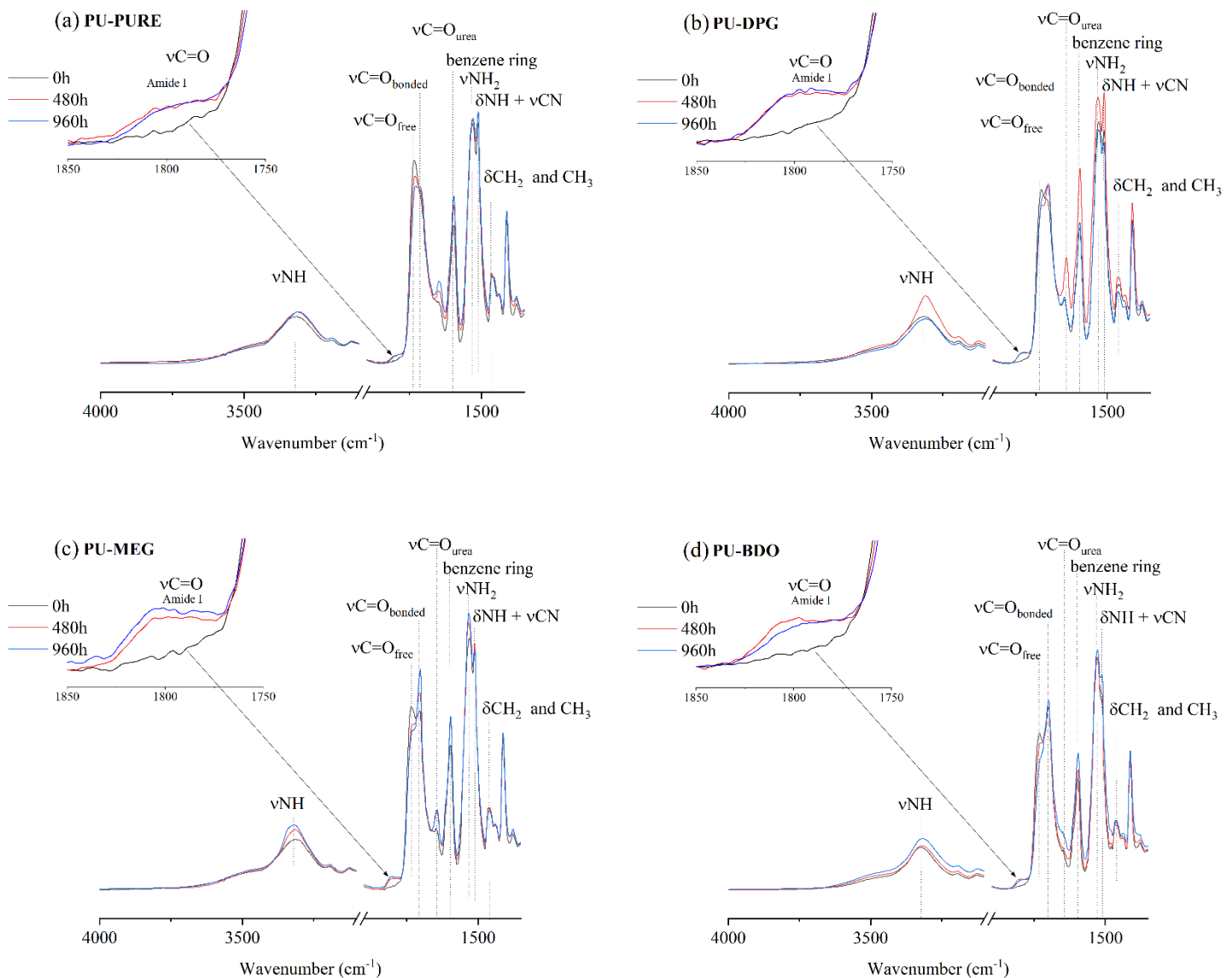


Figure 1. FTIR spectra of the PUs after 0 h (without degradation), 480 h and 960 h of hydrolytic degradation: a) PU-PURE (without chain extender) and different CEs, b) (2-hydroxypropoxy)propano-2-ol (PU-DPG), c) ethane-1,2-diol (PU-MEG) and d) butane-1,4-diol (PU-BDO)

The hydrolytic degradation time effect was studied employing one main band at 1800 cm^{-1} . The appearance amide I group reflects directly the effect associated with the hydrolytic degradation of the soft segment through soybean polyol ester group scission, most probably from triacylglycerol groups[20]. When comparing band ratios $1800:1412\text{ cm}^{-1}$ ($\nu\text{C}=\text{O}_{\text{amide I}}:\delta\text{CH}_2$) bands, it was clear that

the intensity increases by the formation of amide I in the samples with extenders. This behavior can also be inferred by the higher solubility parameter (δ_p) of the samples estimated by Hoftyzer-Van Krevelen method [31] and showed that δ_p is higher for PUs with CEs in the following order: PU-PURE > PU-DPG > PU-BDO > PU-MEG with $\delta_p = 12.31, 13.15, 13.27$ and, 13.79 (cal.cm^{-3})^{1/2}. PU-BDO and PU-MEG show a considerable increase in the amide I group intensity compared to PU-DPG.

The SPUs hydrolytic degradation is polarity dependent on the CE and the capacity to form organized hard domains. The gel content (Table 2) shows that there are practically no changes over time to PU-PURE and in the crosslinking density. Besides, after hydrolytic degradation, the gel content decreases around 20% to PU-MEG and PU-BDO and 50% to PU-DPG. DPG is a chain extender with secondary hydroxyls. Therefore, in the PU formed, there is a reduction in the organization of the HS [5]. In this way, water diffuses more efficiently in the HS, accelerating the degradation rate.

Table 2. Gel content and crosslink density for PU-PURE, PU-BDO, PU-MEG and, PU-DPG: 0, 480 and 960 h

PUs	Gel content (wt.%)			Crosslink density, ν (mol.cm^{-3})		
	0 h	480 h	960 h	0 h	480 h	960 h
PU-PURE	70.5±1.6	63.9±0.3	63.9±0.5	4.1x10 ⁻³ ±0.1x10 ⁻⁴	4.0x10 ⁻³ ±0.2 x10 ⁻⁴	3.3x10 ⁻³ ±0.1 x10 ⁻⁴
PU-DPG	62.4±1.0	39.9±0.3	37.3 ±0.7	4.3x10 ⁻³ ± 0.1x10 ⁻⁴	3.5x10 ⁻³ ±0.5 x10 ⁻⁴	3.0x10 ⁻³ ±0.2 x10 ⁻⁴
PU-MEG	57.9±0.9	45.5±2.1	53.9±1.1	4.9x10 ⁻³ ±0.3 x10 ⁻⁴	4.1x10 ⁻³ ±0.1 x10 ⁻⁴	3.9x10 ⁻³ ±0.1 x10 ⁻⁴
PU-BDO	54.1±1.6	41.5±1.8	47.7±0.7	5.0x10 ⁻³ ±0.1 x10 ⁻⁴	4.2x10 ⁻³ ±0.1 x10 ⁻⁴	3.8x10 ⁻³ ±0.1 x10 ⁻⁴

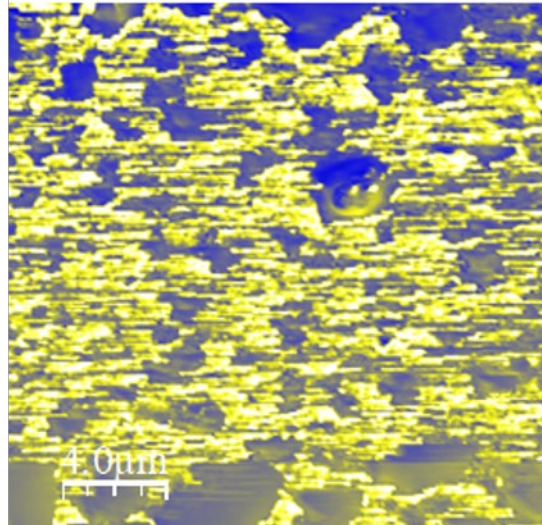
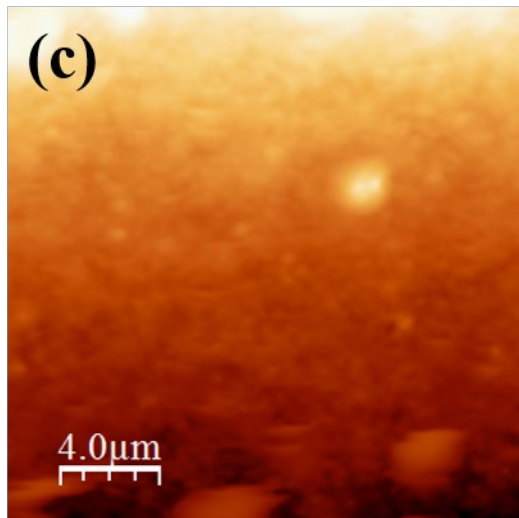
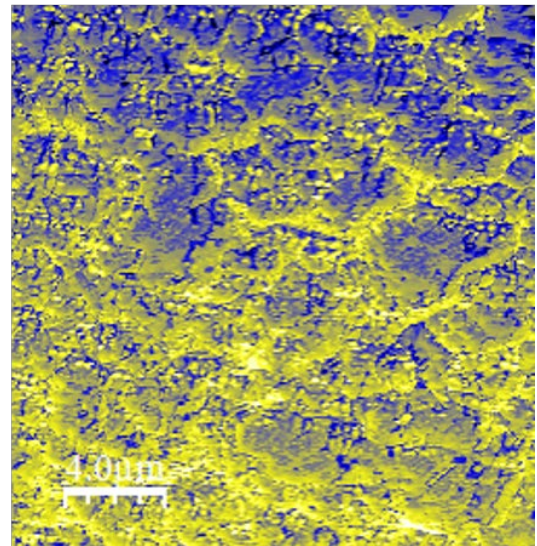
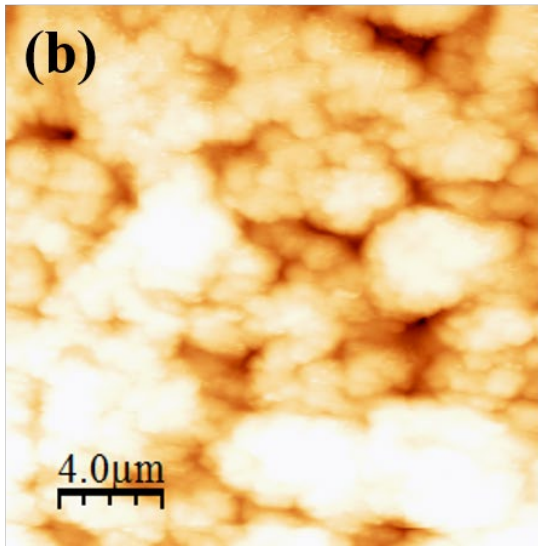
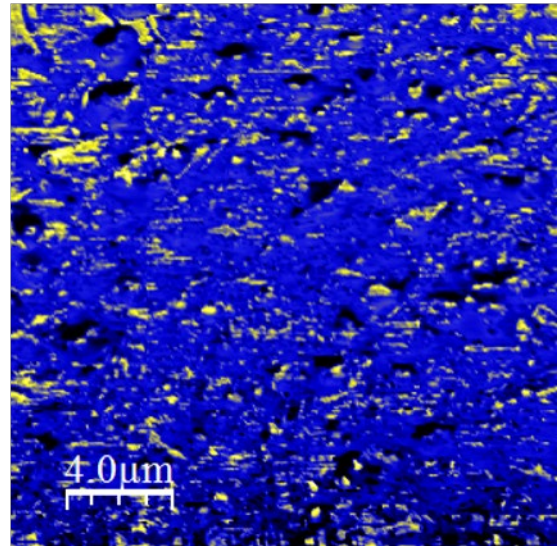
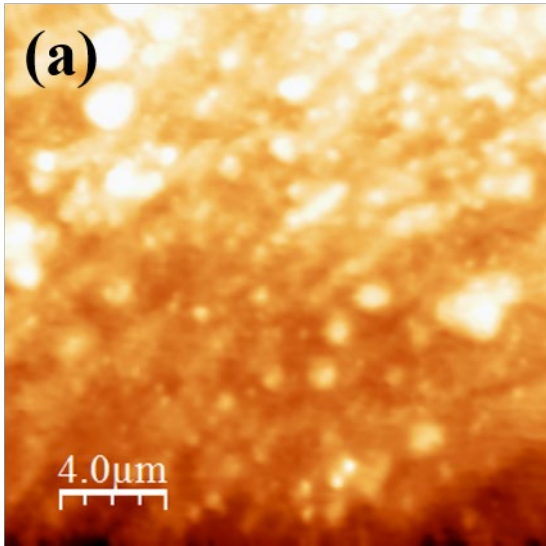
The decrease in gel content values observed in PU-DPG reflects the mixed-phase amount greater of HS dispersed in the soft phase [5]. For the PU with DPG there is an increase in the compatibility between the domains and thus a smaller phase separation since the solubility parameters between the phases become closer. As expected, the reduction of the crosslinking density decreases the degradation times. This reduction results in deterioration of mechanical properties and is strongly

influenced by the type of CEs. Thus, when the HS phase is less compact and allows the diffusion of water, scission of the chain occurs in the HS, which is observed for PU-DPG. Furthermore, a linear increase in density (ρ_p) values with the hydrolysis time is noticed in all PUs, indicating that a more compact phase remains (see supplementary files). Therefore, hydrolysis resistance already indicates the mechanical, dielectric, and thermal properties of SPUs.

Surface energy indicates that changes have occurred in the material's surface after hydrolytic degradation. The SPUs without hydrolytic degradation has surface energy of 68.52 mN/m ($\gamma_L^D = 54.03$ and $\gamma_L^P = 14.49$ mN/m), 69.56 mN/m ($\gamma_L^D = 52.37$ and $\gamma_L^P = 17.19$ mN/m), 70.02 mN/m ($\gamma_L^D = 51.33$ and $\gamma_L^P = 18.70$ mN/m), and 71.27 mN/m ($\gamma_L^D = 50.63$ and $\gamma_L^P = 20.64$ mN/m), for PU-PURE (without chain extender), PU-MEG, PU-BDO, and PU-DPG, respectively. The chain extenders employed increase the PUs surface energy, as expected. In more detail, it can be seen that there was an increase in the polarity of the material and a decrease in the dispersive component value [25].

After 960 h of hydrolytic degradation, there was an increase in the surface energy (polar component) in the PUs: 75.18 mN/m ($\gamma_L^D = 57.67$ and $\gamma_L^P = 17.51$ mN/m), 74.37 mN/m ($\gamma_L^D = 56.08$ and $\gamma_L^P = 18.29$ mN/m), 76.09 mN/m ($\gamma_L^D = 52.83$ and $\gamma_L^P = 23.26$ mN/m), and 77.15 mN/m ($\gamma_L^D = 53.49$ and $\gamma_L^P = 23.67$ mN/m) for the PU-PURE, PU-MEG, PU-BDO, and PU-DPG, respectively. The increase in polarity may be associated with the ester (from polyol) and urethane groups scission ($-\text{COO}$ and $\text{H}_2\text{N}-\text{CO}-\text{R}$) [13]. The scission between the amide groups (from isocyanate) and the carboxylic acid with subsequent amide group I formation, as observed by FTIR analysis (1800 cm^{-1}), also increases the polarity of these materials since these groups have a good affinity with water [31]. Thus, the results obtained agree with the FTIR analysis. Data on surface energy are presented in more detail in Supporting Information (Session 1).

The SPUs morphology was imaged using tapping mode AFM, which allows the simultaneous detection of phase and height features. Fig 2 (a-d) and Fig. 3 (a-d) show the phase (right) and height (left) images of PU-PURE, PU-DPG, PU-MEG, and PU-BDO with hydrolytic degradation effect after 960 h, respectively. Soft domains are anticipated to give dark contrast in the phase imaging (SOP), while hard domains appear as bright areas in height images (MDI/CE)[5].



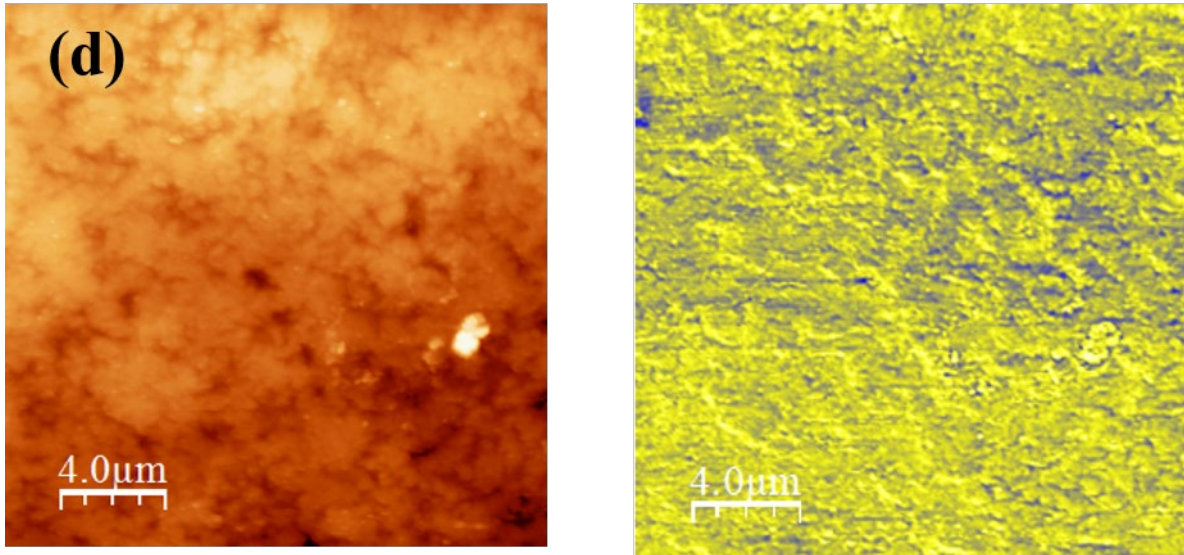
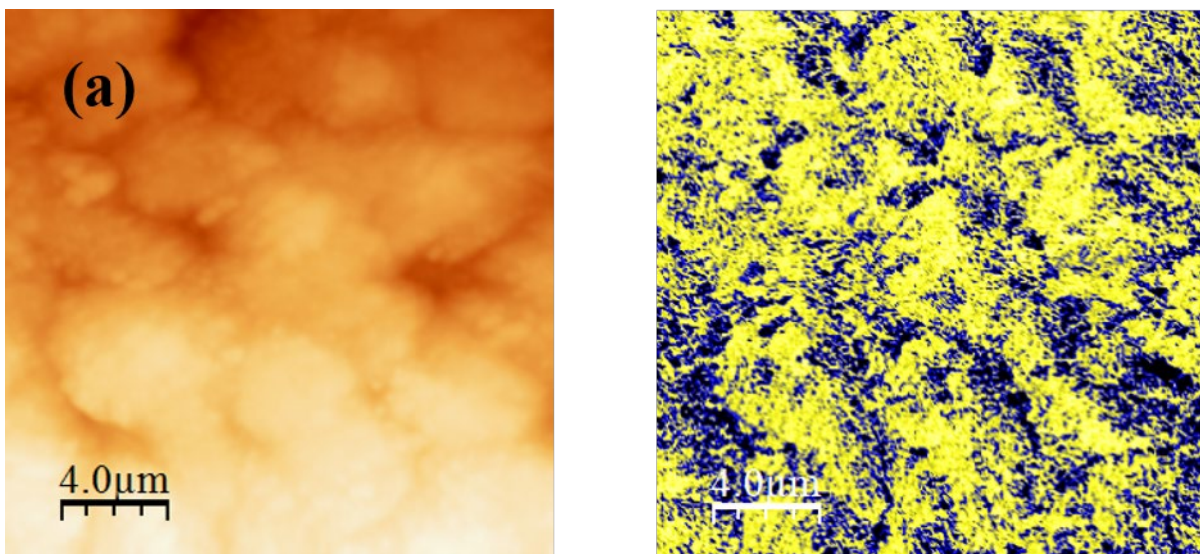


Figure 2. Height (left) and oscillatory phase (right) AFM images without hydrolytic degradation:
 a) PU-PURE (without CE) b) PU-DPG c) PU-MEG d) PU-BDO

The AFM phase image comprises elongated bright structures (yellow - hard phase domain) separated by darker areas (blue - soft phase domain). All SPU micrographs without hydrolytic degradation have a microstructure with a phase separation degree (Fig. 3). The phase separation degree and polarity play an essential role in the hydrolytic degradation behavior. The hydrolytic degradation effect after 480 h (not shown here) on the PU-DPG was observed to increase the formation of well-defined hard segments.



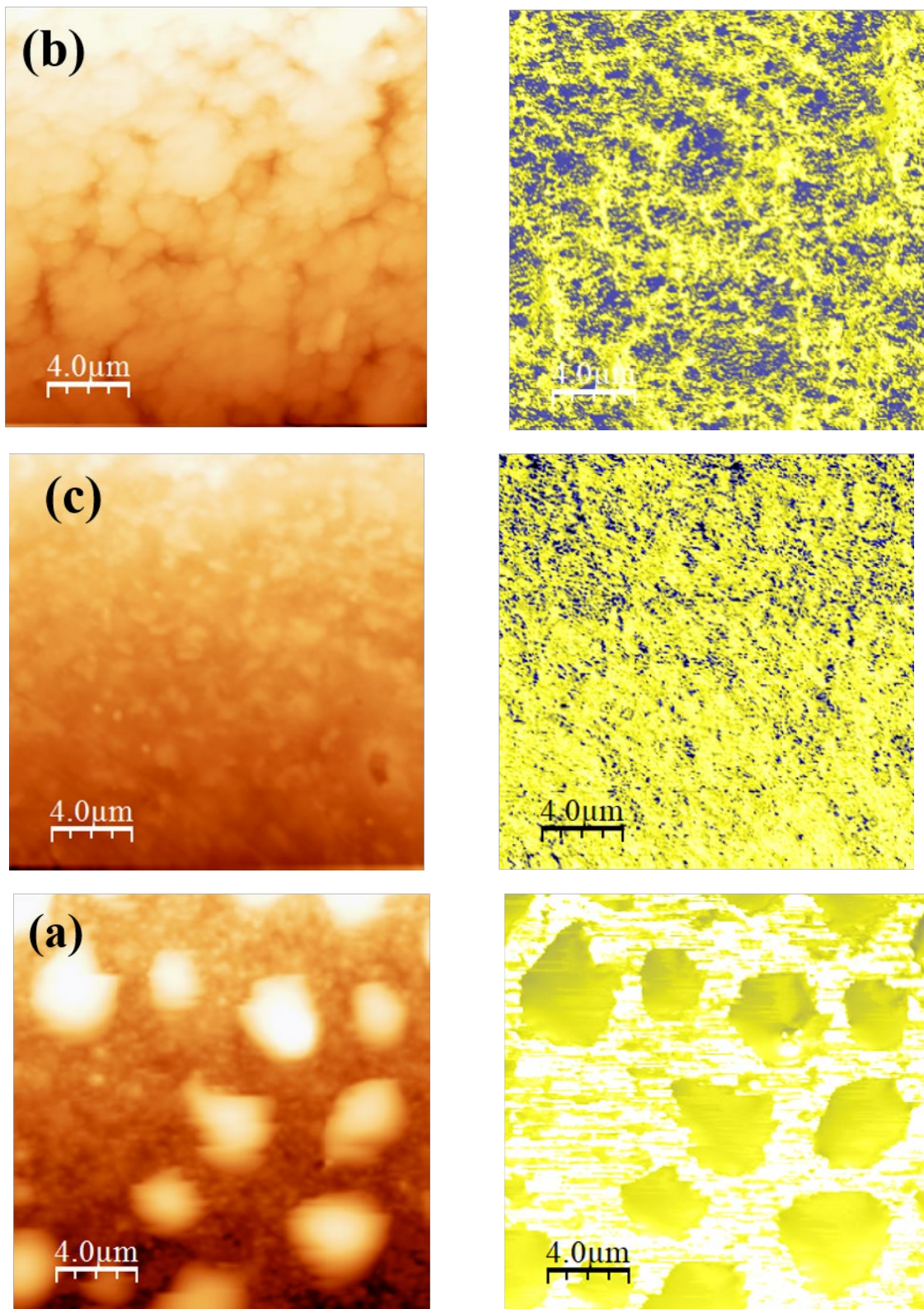


Figure 3. Height (left) and oscillatory phase (right) AFM images after 960 h hydrolytic degradation: a) PU-PURE (without CE) b) PU-DPG c) PU-MEG d) PU-BDO

After 960 h of hydrolytic degradation all SPUs with CEs show a loss of material and that a more rigid phase in the topology, which refers to the HS. This behavior can make the material harder and more brittle as the ratio of rigid/flexible segments changes. On the other hand, the chain scission and subsequent removal of the soft segment that started mainly in the ester bonds with the triacylglycerol of the soy polyol (amorphous domain) show evidence that this region is more susceptible to chain scission. These observations are supported by the hydrolytic degradation rate of the ester group being twice as high as that of urethane and the results shown in the literature [3, 13]. Thus, it was noted that the appearance of globular domains in the case of PU-BDO (Fig. 3d). This may indicate that depending on the extender used in the synthesis and on the degree of phase separation of the PU, the chain scission in the SS can be of greater or lesser intensity. Thus, when the HS is organized, it reduces water diffusion and can often minimise hydrolytic degradation. In contrast, a relative increase in rigid domains can weaken the material.

The storage modulus (E') behavior vs. temperature for PU-PURE, PU-MEG, PU-BDO, and PU-DPG after 0h, 480 h, and 960 h of hydrolytic degradation showed solid-like behavior for all PUs. It was noted that the vitreous region runs up to close to 0°C while above 50 °C, the beginning of the elastic plateau is observed. It would generally be expected that hydrolytic degradation would produce a reduction in molecular weight, entanglements, and crosslink density, as it is commonly observed in polyurethanes [3, 4, 13, 20]. However, there is a relative change in the HS and SS due to the scission of the flexible phase ester groups. Therefore, mechanical properties may or may not be reduced due to rigidity. For better visualization of this effect, relative modulus (E_i/E_0) values for 23 °C and 100 °C were compared as a function of hydrolysis time (Fig. 4).

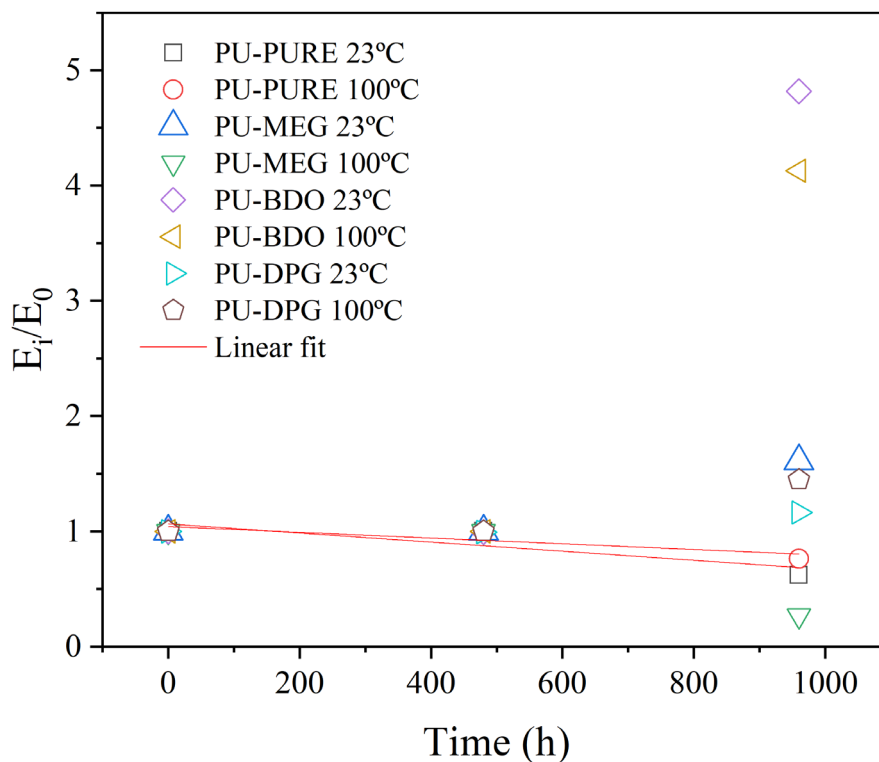


Figure 4. Relative moduli E_i/E_0 as a function of hydrolysis time for PU-PURE, PU-MEG, PU-DPG, and PU-BDO. The lines refer to the linear fit (guide) of the relative modulus of the PU-PURE sample at 23 °C and 100 °C.

In all samples, it is clear that the hydrolysis time of 480 h practically did not affect the mechanical behavior. However, with the time of 960 h, a reduction of the modulus for PU-PURE and PU-MEG is noticed. The use of CEs, in general, showed the formation of more rigid polymers. As mentioned before, as there is a change in the relative amount in the fraction between rigid/flexible segments, there is an increase in the stiffness of the PU. Although additional crosslinks could be formed due to urea groups, this was not evident in the gel content measurements and crosslink density via swelling. It is considering that there is already a percolated structure of rigid and flexible domains in the initial composition, the hydrolysis of the flexible phase-only increases the relative fraction of the rigid phase, which increases rigidity. This is most evident in PUs with a more organized rigid phase structure (BDO), with a tendency to increase the modulus at 23 °C and 100 °C.

The macromolecular motions associated with a hard-domain glass transition temperature (T_{gH}) and soft-domain glass transition temperature (T_{gS}) and Schatzki mechanism for PU-PURE, PU-BDO, PU-MEG, and PU-DPG after 480 h and 960 h hydrolytic degradation were obtained from the peaks of the $\tan \delta$ curves by DMA and DRS. The corresponding spectra at 1Hz are shown in Fig. 5, 6, and 7, respectively. The PU-PURE showed a low T_{gS} (239 K) compared to other PUs. The PUs with CEs shifted the T_{gS} to around 245 K, while the T_g of pure soybean oil polyol was ~ 80 °C[21].

The T_{gS} increased in PUs with CEs, indicating the phase-mixing between hard and soft domains. The T_{gH} decreases systematically with increasing methylene sequences ($-\text{CH}_2$) [6]. The PU-BDO and PU-MEG follow this trend, while the PU-DPG does not follow this behavior due to secondary hydroxyl groups and heteroatom in its structure [5].

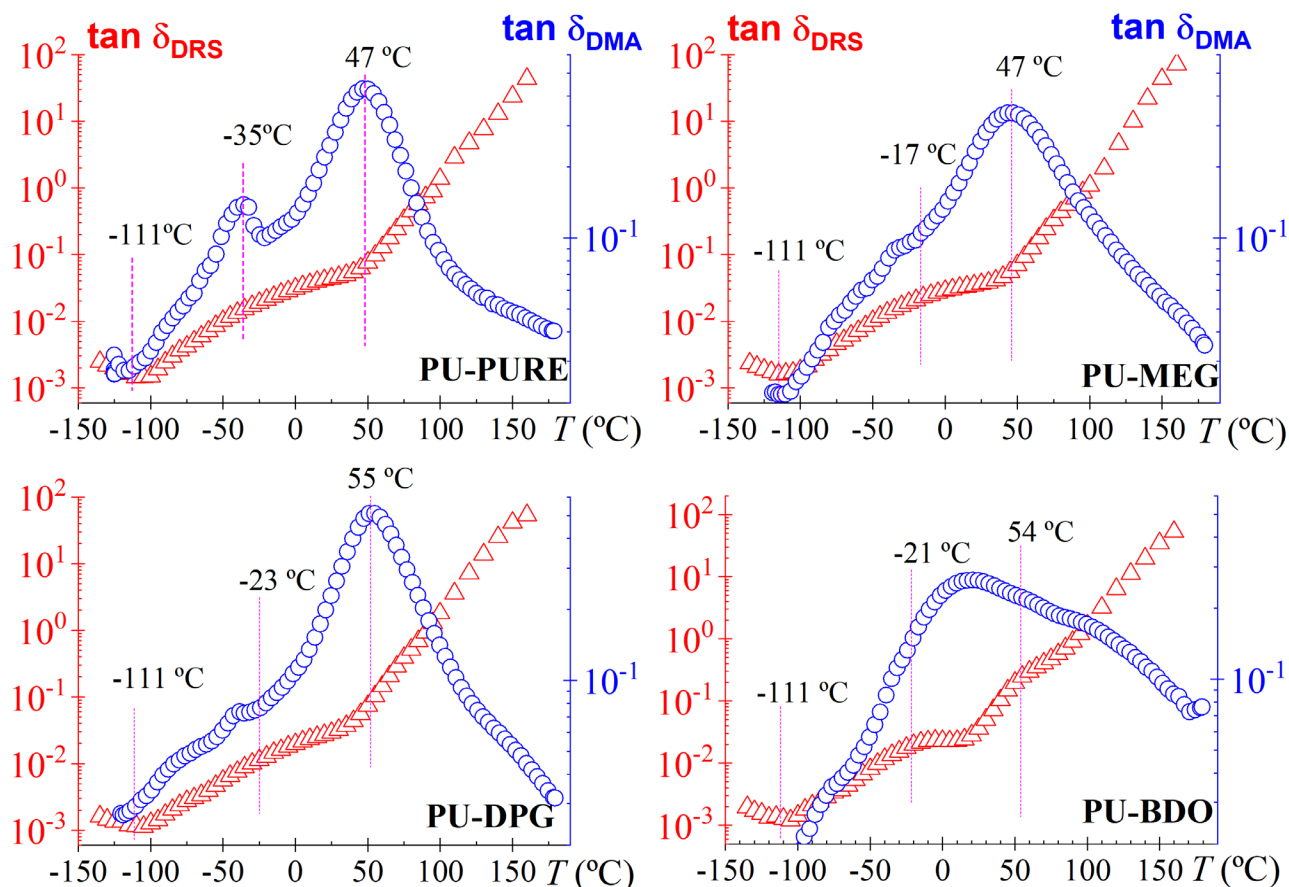


Figure 5. $\tan \delta$ vs. temperature at 1Hz: PU-PURE, PU-MEG, PU-DPG, and PU-BDO without hydrolytic degradation.

Fig. 6 shows the T_g behavior for all SPUs after 480 h of the hydrolysis. The decrease in T_{gS} came about mainly due to the cleavage of the SOP triacylglycerol ester bonds (amorphous domain) and hydrogen bonds (intra and inter-molecular) in the polymer structure. In general, it was noticed that T_{gS} and T_{gH} are wider after degradation; this is due to the formation of chains domains with heterogeneous sizes. Thus, the macromolecular mobility spectrum becomes broader. Furthermore, as the session starts with the flexible segment, which is less compact and has more easily hydrolyzable groups, the fragments generated in this domain are more easily removed [13].

PU-PURE

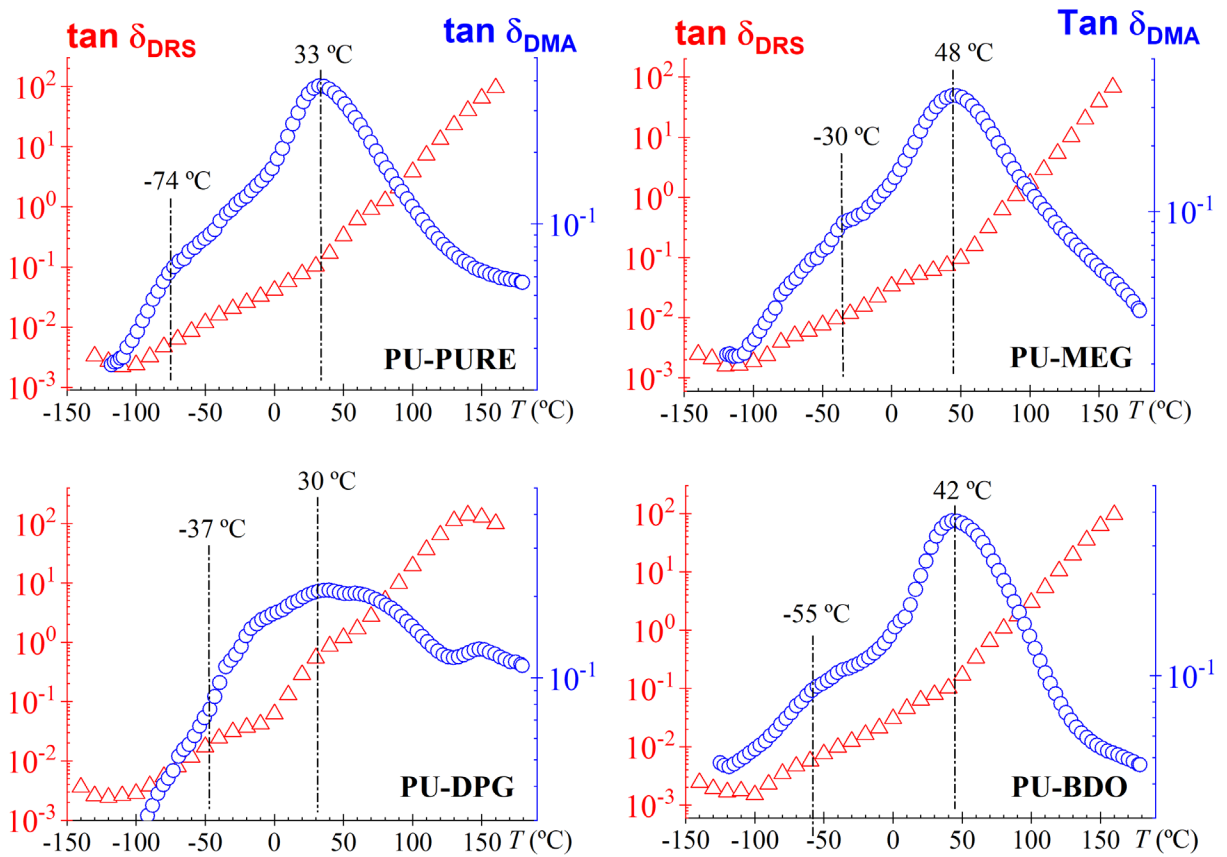


Figure 6. $\tan \delta$ vs. temperature at 1Hz after 480 h hydrolytic degradation of PU-PURE, PU-MEG, PU-DPG and PU-BDO.

Hydrolytic degradation effect after 960 h (Fig. 7) for all SPUs with CEs the T_{gS} decreased (around -72 to -82 °C). There was a loss of mobility due to removing part of the flexible segment since the chain scission starts in this segment. It seems to be a balance between linkages scission. For PU-PURE, chain cleavage always occurs in the ester groups and urethane. However, for PUs with chain extenders, this rule is not valid, as there may be the formation of small-organized domains that result in less water diffusion. For these PUs, we observed that BDO and MEG form organized regions, while DPG induces the formation of an amorphous structure [5].

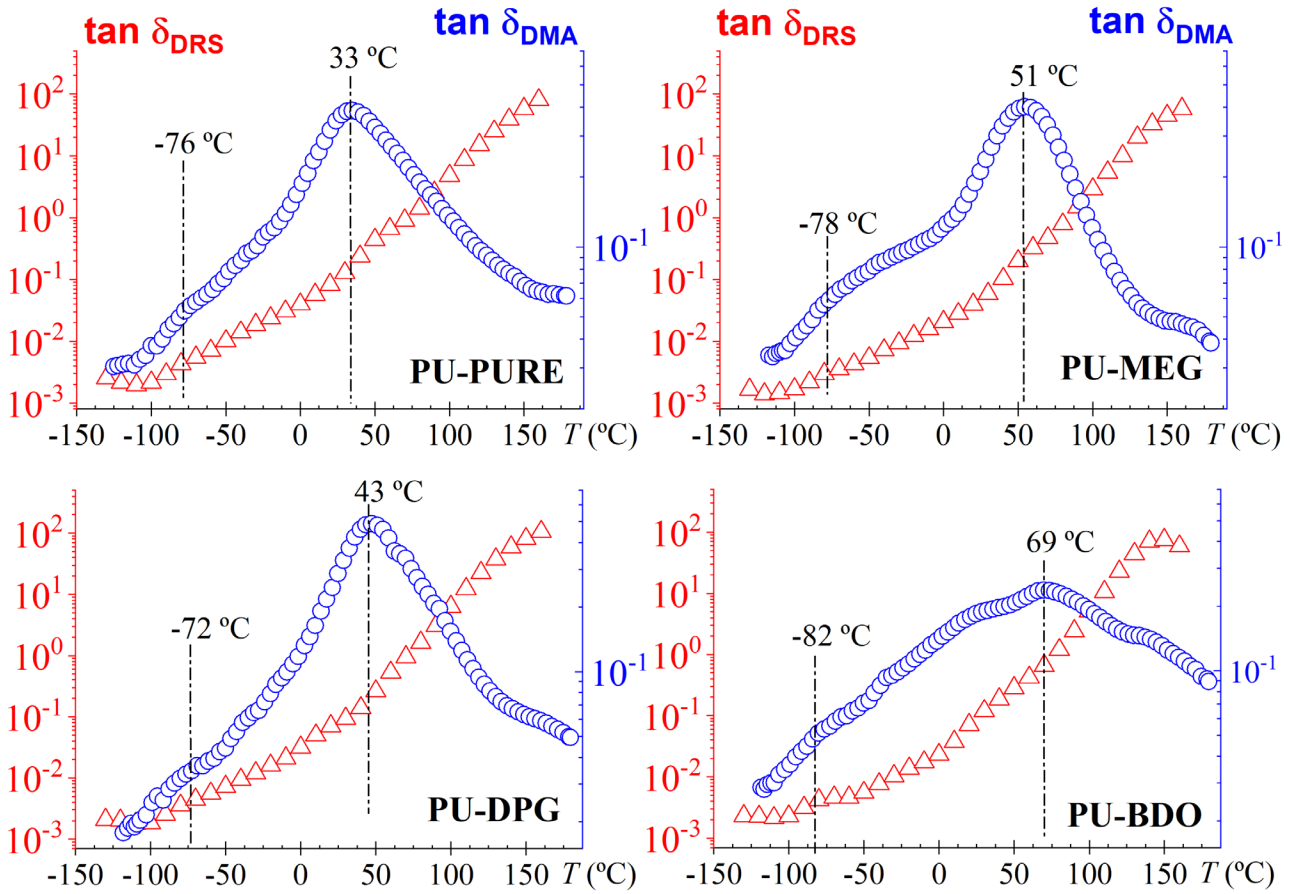


Figure 7. $\tan \delta$ vs. temperature at 1Hz after 960 h hydrolytic degradation of PU-PURE, PU-MEG, PU-DPG, and PU-BDO.

Consequently, variations in the free volume are due to the type of structure obtained. This modulates the diffusion of water into the polymeric structure, and a good balance of mechanical properties can be obtained. Thus, in situations where the rigid segment is compact such as PU-BDO, the T_{gH} increased from 30 °C to 69 °C. This happens simply because there is a local change between the rigid and flexible phases. Therefore, this material will be harder and more brittle with a loss of mechanical properties.

The mobility present in the mechanical and electrical fields of these SPUs appears in more detail by DRS analysis. At low temperatures, two secondary transitions appear: γ -transitions and β -transition attributed to the small group's rotational motions in the polyol fatty acid chains. This transition is associated with the reorientation motions of water molecules and is present in a wide variety of water-containing systems. In the case of hydrated polymers, the relaxation is also likely to involve local motions of the polymer chain segments where the water molecules are attached [32]. In general, γ and β are little affected by the rigid phase; however, they depend on the number of dangling groups [32, 33]. At intermediate temperatures, two processes are observed, the α -relaxation,

associated with the cooperative segmental movement of the matrix rich in soft segments, and the I process, which is associated with the rigid segments that appear at high temperature/low frequency [32]. Finally, a typical Maxwell-Wagner-Sillars (MWS) relaxation interface heterogeneous system is observed at high temperatures [21, 32]. Fig. 8 (a-d) shows the temperature dependence of $\tan \delta$ at 1039 Hz for PU-PURE (a), PU-MEG (b), PU-DPG (c), and PU-BDO (d) by DRS before and after 960 h of the hydrolysis. To reduce the error associated with the measurement of the thickness of the samples, we are representing the temperature dependence of $\tan \delta$ ($\delta = \epsilon''/\epsilon'$), since this dielectric constant is independent of the geometry of the sample. The $\tan \delta$ curves show a γ peak at -111°C relating to the crankshaft motions mechanism and -60°C relaxations associated with β -transition. In this temperature range, all PUs show the γ and β transitions and continuous increase of the increase in $\tan \delta$ with temperature.

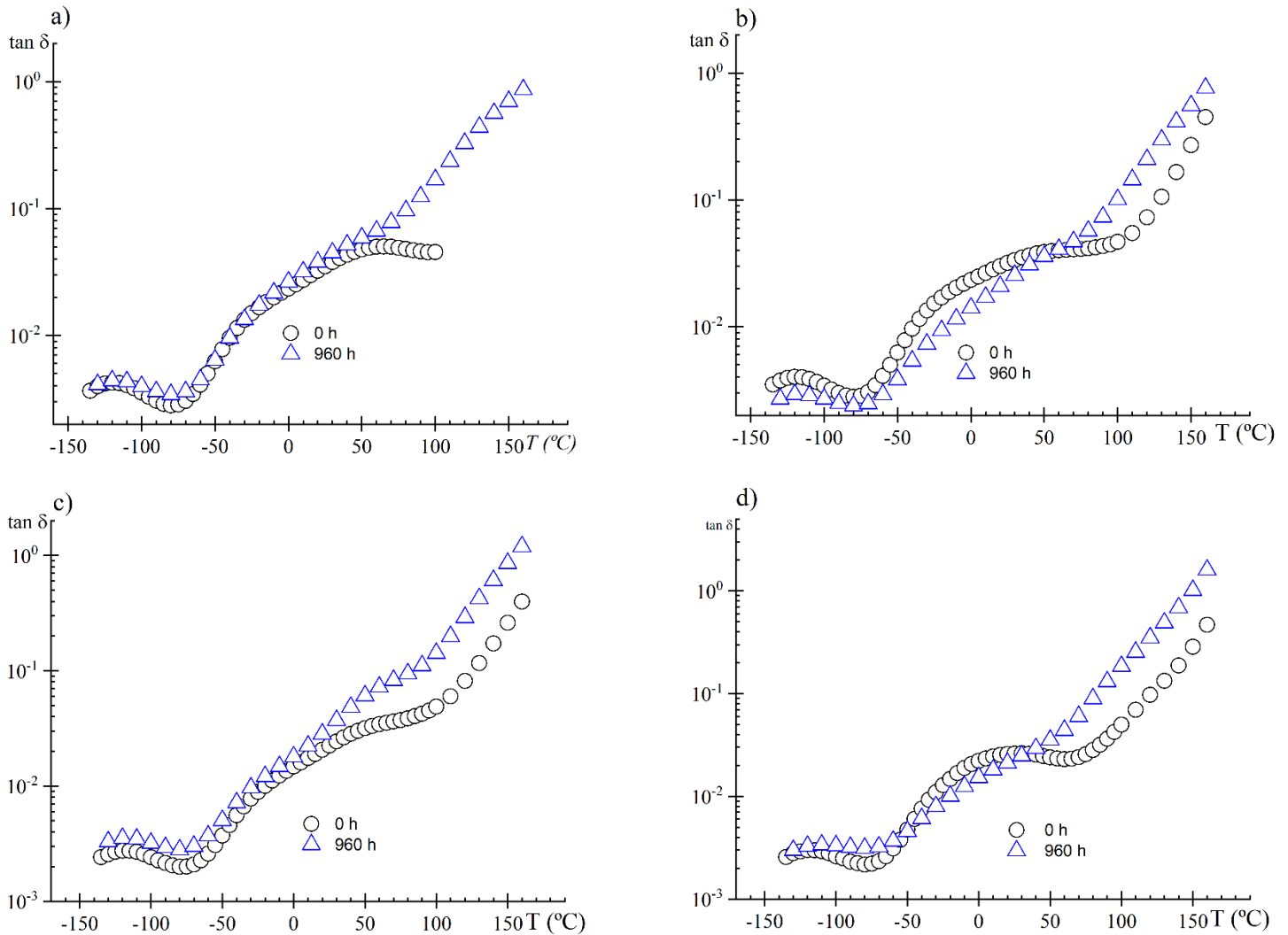


Figure 8. $\tan \delta$ vs. temperature at 1039 Hz for a) PU-PURE, b) PU-MEG, c) PU-DPG and d) PU-BDO.

In general, in all samples after hydrolysis, an increase in $\tan \delta$ values was noted compared to samples before degradation. This increase is associated with greater mobility (increase in ϵ'') promoted by the chain scission, mainly in the flexible phase. As local mobility increases, the molecules can polarize more quickly concerning the electrical field. For the non-hydrolyzed sample, the $\tan \delta$ values are smaller, which indicates a greater dielectric strength [34]. Note that the transition region β is more affected because groups such as ester are undergoing chain scission due to prolonged exposure to water. In this way, a wider distribution of the $\tan \delta$ values in the transition is noticed.

In particular, the γ -transition is related to the ether-based PU crankshaft motions of the ether oxygen. This transition generally has activation energy ~ 43 kJ/mol [32]. The polyol used in this work was obtained from a ring-opening reaction of epoxidized soybean oil with diethylene glycol by microwave-assisted reactions. This process was used because diethylene glycol has a high dielectric loss [21]. Thus, we are also interested in this region's effects since this type of material can show chain mobility at low temperatures.

The dielectric constant (ϵ') behavior in the γ -transition around -120 °C for PU-PURE, PU-MEG, PU-DPG and PU-BDO before and after hydrolysis do not show here any significant change in samples with CEs. In the PU-PURE, a slight shift in ϵ' was observed. However, in all PUs with CEs, as already noted, degradation occurs initially in the flexible phase. Thus, if we consider that PU-PURE forms few segregated and polydispersed domains [5], the hydrolytic degradation is expected to be smaller and therefore does not increase the ϵ'' . On the other hand, when extenders such as DPG, MEG, and BDO are used, there is an amount of rigid phase that gets mixed ($\sim 0.12\%$), and therefore, by increasing the polarity and being miscible in water, they can act as nucleating regions for chain scission. These observations are consistent with the work of Ourique and coworkers by studying the degradation of PUs from soybean oil used as metallic coatings in salt spray [16]. They observed that when a rich urea phase was formed by adding 3-(aminopropyl)trimethoxysilane, the hydrolysis occurred in a shorter time, resulting in coatings with inferior properties.

The loss permittivity (ϵ'') in the γ -transition region at -120 °C and -130 °C for PU-PURE, PU-MEG, PU-DPG and PU-BDO after 960 h of hydrolytic degradation are shown in Fig. 9 (a-d). For all SPUs, the increase in ϵ'' at low frequencies is a conductivity result due to the free charge motion effects within the polymeric material [35]. This behavior is typical of polyurethanes based on vegetable oils, such as castor oil, which has pendant chains in its main chain that increase the mobility of the chains [36]. The frequency with which the relaxation peak γ appears, for all PUs, does not significantly change. PU-PURE did not show changes in dipole mobility in the γ -transition region.

However, for MEG and BDO, there is a significant change in samples with MEG and BDO. These samples have a reduction in mobility due to the change in the rigid/flexible segment fraction, as observed in the DMA results. These results are also supported by the observations of the FTIR bands in the C=O region, which is sensitive to phase separation [5]. Thus, the reduction in mobility is related to the change in the ratio between flexible and rigid phases, and is evident in PUs with more compact domains by reducing the value of ϵ'' .

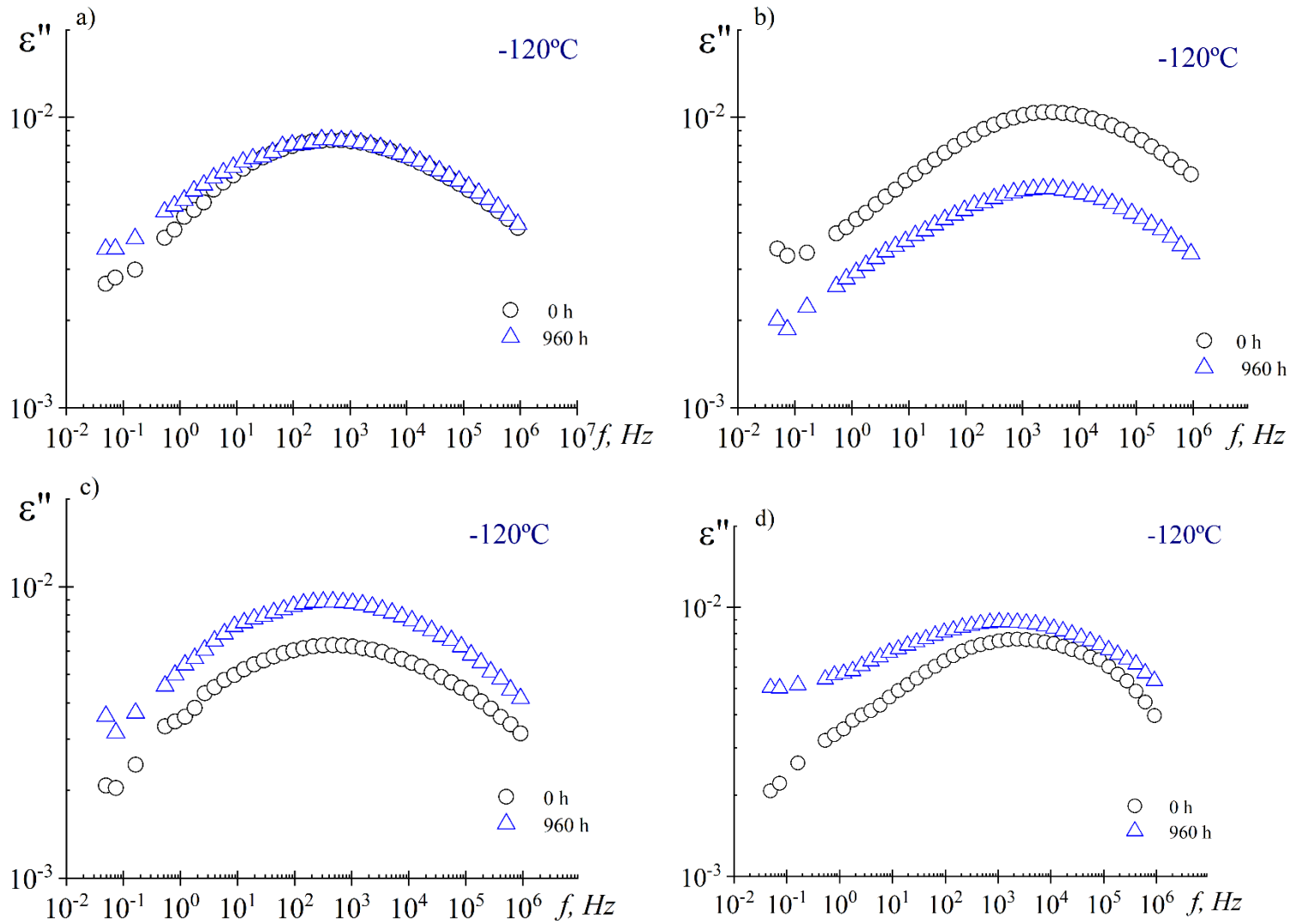


Figure 9. Frequency dependence of loss permittivity (ϵ'') in the γ -transition of a) PU-PURE, b) PU-MEG, c) PU-DPG and d) PU-BDO

4. CONCLUSIONS

This article evaluates the hydrolytic degradation effect at different times up to 960 h of soybean-polyurethanes synthesized with different chains (BDO, MEG, and DPG). The physico-

chemical, morphological, dielectric, and solid-viscoelastic properties have been evaluated. Besides, the DMA and DRS combination analysis have been correlated with the mobility response in the mechanical and electrical fields. The CEs form hard compact domains increasing physical crosslinking, polarity, and surface energy, thus reducing the dispersive component. In summary, when CEs provide increased water diffusion in the PU, there is an acceleration in chain scission, as evidenced by the reduction in gel content and crosslink density. For CEs that form compact, rigid domains, a change in the ratio between rigid/flexible segments is noticed due to the greater selectivity to hydrolysis by the ester groups of the flexible domain. This change in the proportion between the domains changes the phase separation is evident in the phase morphology and decreasing the intensity of the C=O_{free} band at 1730 cm⁻¹, while increasing the intensity of C=O_{bonded} at 1710 cm⁻¹ indicated a higher phase separation degree. The new bands of the urea (1640 cm⁻¹) and amide (1800 cm⁻¹) groups were formed during hydrolytic degradation. After 960 h, the T_{gS} decreased, while the T_{gH} was practically unchanged. The hydrolytic degradation alters the rigid/flexible domains ratio, resulting in a high relative module. These results allow a better understanding of the hydrolytic degradation of polyurethanes based on soybean oil concerning structure and properties. With this, it is possible to evaluate which best set of monomers can be used in applications that require hydrolytic stability.

ACKNOWLEDGEMENTS

The authors thank the financial support from the Brazilian Agency Coordenação de Aperfeiçoamento de Pessoal de Nível Superior (CAPES), CAF and OB are National Council for Scientific and Technological Development (CNPq) fellows (grant number 308567/2018-8 and 305814/2021-4). CMG and MJS thank the Spanish Ministerio de Economía y Competitividad (RTI2018-093711-B-100) for partial financial help. A. C. acknowledges financial support from xxx (AEI/FEDER, UE).

DATA AVAILABILITY

The raw data needed to reproduce these findings can be shared if requested from the authors.

REFERENCES

[1] R. Raghavachar, G. Sarnecki, J. Baghdachi, J. Massingill, Cationic, thermally cured coatings using epoxidized soybean oil, *Journal of Coatings Technology* 72(909) (2000) 125-133.

- [2] J. John, M. Bhattacharya, R.B. Turner, Characterization of polyurethane foams from soybean oil, *Journal of Applied Polymer Science* 86(12) (2002) 3097-3107.
- [3] P.-Y. Le Gac, D. Choqueuse, D. Melot, Description and modeling of polyurethane hydrolysis used as thermal insulation in oil offshore conditions, *Polymer Testing* 32(8) (2013) 1588-1593.
- [4] A. Bardin, P.Y. Le Gac, H. Bindi, B. Fayolle, Relationships between molar mass and fracture properties of segmented urethane and amide copolymers modified by chemical degradation, *Journal of Polymer Science* 58(22) (2020) 3170-3182.
- [5] D. Favero, V. Marcon, C.A. Figueroa, C.M. Gómez, A. Cros, N. Garro, M.J. Sanchis, M. Carsí, O. Bianchi, Effect of chain extender on the morphology, thermal, viscoelastic, and dielectric behavior of soybean polyurethane, *Journal of Applied Polymer Science* 138(27) (2021) 50709.
- [6] G. Oertel, L. Abele, *Polyurethane handbook: chemistry, raw materials, processing, application, properties*, 1994.
- [7] R.L. Shogren, Z. Petrovic, Z. Liu, S.Z. Erhan, Biodegradation behavior of some vegetable oil-based polymers, *Journal of Polymers and the Environment* 12(3) (2004) 173-178.
- [8] C. Schollenberger, F. Stewart, Thermoplastic polyurethane hydrolysis stability, *Journal of Elastoplastics* 3(1) (1971) 28-56.
- [9] D. Macocinschi, D. Filip, M.F. Zaltariov, C.D. Varganici, Thermal and hydrolytic stability of silver nanoparticle polyurethane biocomposites for medical applications, *Polymer Degradation and Stability* 121 (2015) 238-246.
- [10] W. Lei, C. Fang, X. Zhou, Y. Cheng, R. Yang, D. Liu, Morphology and thermal properties of polyurethane elastomer based on representative structural chain extenders, *Thermochimica Acta* 653 (2017) 116-125.
- [11] D.W. Brown, R.E. Lowry, L.E. Smith, Kinetics of hydrolytic aging of polyester urethane elastomers, *Macromolecules* 13(2) (1980) 248-252.
- [12] C. Hepburn, Trends in polyurethane elastomer technology, *Iranian Journal of Polymer Science and Technology* 1(2) (1992).
- [13] F. Xie, T. Zhang, P. Bryant, V. Kurusingal, J.M. Colwell, B. Laycock, Degradation and stabilization of polyurethane elastomers, *Progress in Polymer Science* 90 (2019) 211-268.
- [14] S.D. Bote, R. Narayan, Synthesis of Biobased Polyols from Soybean Meal for Application in Rigid Polyurethane Foams, *Industrial & Engineering Chemistry Research* 60(16) (2021) 5733-5743.
- [15] P.A. Ourique, J.M.L. Gril, G.W. Guillaume, C.H. Wanke, S.G. Echeverrigaray, O. Bianchi, Synthesis and characterization of the polyols by air oxidation of soybean oil and its effect on the morphology and dynamic mechanical properties of poly(vinyl chloride) blends, *Journal of Applied Polymer Science* 132(24) (2015).

- [16] P.A. Ourique, I. Krindges, C. Aguzzoli, C.A. Figueroa, J. Amalvy, C.H. Wanke, O. Bianchi, Synthesis, properties, and applications of hybrid polyurethane–urea obtained from air-oxidized soybean oil, *Progress in Organic Coatings* 108 (2017) 15-24.
- [17] Z.S. Petrović, Polyurethanes from vegetable oils, *Polymer Reviews* 48(1) (2008) 109-155.
- [18] N. Sangeetha, *BIODEGRADATION OF POLYURETHANE COMPOSITES*, Laxmi Book Publication, Raleigh, 2018.
- [19] J. Zhang, J. Chen, M. Yao, Z. Jiang, Y. Ma, Hydrolysis-resistant polyurethane elastomers synthesized from hydrophobic bio-based polyfarnesene diol, *Journal of Applied Polymer Science* 136(25) (2019) 47673.
- [20] M. Carme Coll Ferrer, D. Babb, A.J. Ryan, Characterisation of polyurethane networks based on vegetable derived polyol, *Polymer* 49(15) (2008) 3279-3287.
- [21] D. Favero, V.R. Marcon, T. Barcellos, C.M. Gómez, M.J. Sanchis, M. Carsí, C.A. Figueroa, O. Bianchi, Renewable polyol obtained by microwave-assisted alcoholysis of epoxidized soybean oil: Preparation, thermal properties and relaxation process, *Journal of Molecular Liquids* 285 (2019) 136-145.
- [22] M.F. Pacheco, O. Bianchi, R. Fiorio, A.J. Zattera, M. Zeni, M. Giovanela, J.S. Crespo, Thermal, chemical, and morphological characterization of microcellular polyurethane elastomers, *Journal of Elastomers & Plastics* 41(4) (2009) 323-338.
- [23] M. Jayabalan, P.P. Lizymol, V. Thomas, Synthesis of hydrolytically stable low elastic modulus polyurethane-urea for biomedical applications, *Polymer international* 49(1) (2000) 88-92.
- [24] D.K. Owens, R. Wendt, Estimation of the surface free energy of polymers, *Journal of applied polymer science* 13(8) (1969) 1741-1747.
- [25] L.D. Agnol, F.T.G. Dias, N.F. Nicoletti, D. Marinowic, S. Moura e Silva, A. Marcos-Fernandez, A. Falavigna, O. Bianchi, Polyurethane tissue adhesives for annulus fibrosus repair: mechanical restoration and cytotoxicity, *Journal of biomaterials applications* 34(5) (2019) 673-686.
- [26] H.S. Lee, Y.K. Wang, S.L. Hsu, Spectroscopic analysis of phase separation behavior of model polyurethanes, *Macromolecules* 20(9) (1987) 2089-2095.
- [27] L.-S. Teo, C.-Y. Chen, J.-F. Kuo, Fourier transform infrared spectroscopy study on effects of temperature on hydrogen bonding in amine-containing polyurethanes and poly (urethane– urea) s, *Macromolecules* 30(6) (1997) 1793-1799.
- [28] T. Pretsch, I. Jakob, W. Müller, Hydrolytic degradation and functional stability of a segmented shape memory poly (ester urethane), *Polymer Degradation and Stability* 94(1) (2009) 61-73.
- [29] M.M. Coleman, D.J. Skrovanek, J. Hu, P.C. Painter, Hydrogen bonding in polymer blends. 1. FTIR studies of urethane-ether blends, *Macromolecules* 21(1) (1988) 59-65.

- [30] J. Hocker, Structural investigation of polyurethanes: Infrared spectroscopic investigations of monomeric and polymeric N, N'-diaryl ureas, *Journal of Applied Polymer Science* 25(12) (1980) 2879-2889.
- [31] D.W. Van Krevelen, K. Te Nijenhuis, *Properties of polymers: their correlation with chemical structure; their numerical estimation and prediction from additive group contributions*, Elsevier, Oxford, 2009.
- [32] A.M. Castagna, D. Fragiadakis, H. Lee, T. Choi, J. Runt, The Role of Hard Segment Content on the Molecular Dynamics of Poly(tetramethylene oxide)-Based Polyurethane Copolymers, *Macromolecules* 44(19) (2011) 7831-7836.
- [33] W. Yu, M. Du, D. Zhang, Y. Lin, Q. Zheng, Influence of Dangling Chains on Molecular Dynamics of Polyurethanes, *Macromolecules* 46(18) (2013) 7341-7351.
- [34] B. Redondo-Foj, P. Ortiz-Serna, M. Carsí, M.J. Sanchis, M. Culebras, C.M. Gómez, A. Cantarero, Electrical conductivity properties of expanded graphite–polycarbonatediol polyurethane composites, *Polymer International* 64(2) (2015) 284-292.
- [35] M.J. Sanchis, M. Carsí, C.M. Gómez, M. Culebras, K.N. Gonzales, F.G. Torres, Monitoring molecular dynamics of bacterial cellulose composites reinforced with graphene oxide by carboxymethyl cellulose addition, *Carbohydrate Polymers* 157 (2017) 353-360.
- [36] S. Oprea, O. Potolinca, V. Oprea, Dielectric properties of castor oil cross-linked polyurethane, *High Performance Polymers* 23(1) (2011) 49-58.

SUPPLEMENTARY FILES FOR:

EFFECT OF CHAIN EXTENDERS ON THE HYDROLYTIC DEGRADATION OF SOYBEAN POLYURETHANE

Diana Favero¹, Victória Marcon¹, Lucas Dall Agnol¹, Clara M. Gómez², Ana Cros², Nuria Garro², Maria J. Sanchis³, Marta Carsí⁴, Carlos A. Figueroa¹, Otávio Bianchi^{1,5*}

¹ *Postgraduate Program in Materials Science and Engineering (PGMAT), University of Caxias do Sul (UCS), Caxias do Sul, RS, Brazil;*

² *Instituto de Ciencia de los Materiales, Universidad de Valencia, 46980 Paterna, València, Spain;*

³ *Department of Applied Thermodynamics, Institute of Electric Technology, Universitat Politècnica de València, Spain;*

⁴ *Department of Applied Thermodynamics, Instituto de Automática e Informática Industrial, Universitat Politècnica de Valencia, 46022 Valencia, Spain;*

⁵ *Department of Materials Engineering (DEMAT), Federal University of Rio Grande do Sul (UFRGS), Porto Alegre, RS, Brazil.*

***Corresponding author.** Tel: +55 (54) 984030958; E-mail address: otavio.bianchi@gmail.com (Bianchi O.)

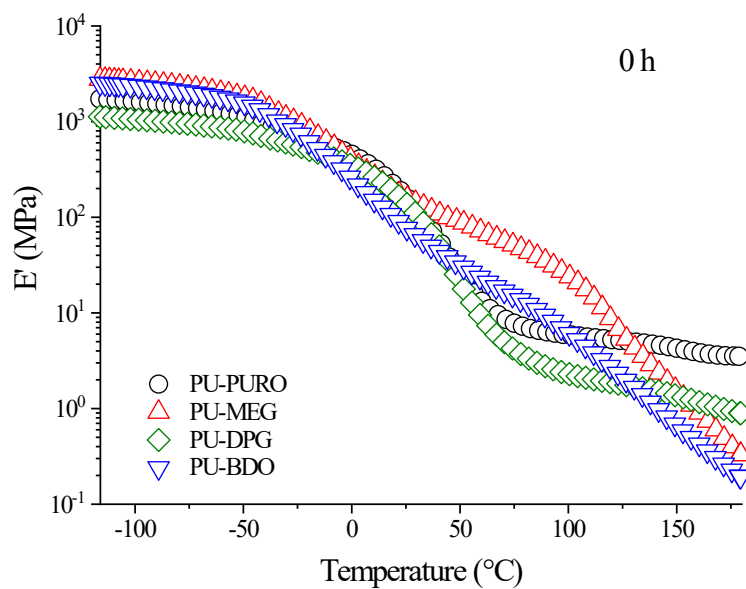
Table S1 shows the contact angle values for the polyurethane films at times of 0, 480, and 960h of hydrolysis in water, glycerin, dimethylformamide, and hexadecane are presented. These values were used to estimate surface energy[1]. Table S2 shows density values that were made following ASTM D 792. The storage modules, E' as a function of temperature for samples before and after hydrolysis are shown in Fig. s1, s2, and s3. In Fig. S4 the frequency dependence of dielectric constant (ϵ') in the γ -transition of a) PU-PURE, b) PU-MEG, c) PU-DPG, and d) PU-BDO are shown.

Table S1. Contact angles (θ , °C) and surface free energy (γ_s) of the solid surfaces, including dispersive (γ_s^D) and polar (γ_s^P) contributions

Solid surfaces	Contact Angle (θ , °C)				Surface free energy (mN/m)			R^2	
	Water	Glycerin	Dimethylformamide	Hexadecane	γ_s	γ_s^D	γ_s^P		
0 h	PU-PURE	107.9 ± 0.8	87.0 ± 0.5	49.0 ± 0.6	32.9 ± 0.5	68.52	54.03	14.49	0.987
	PU-MEG	101.0 ± 0.7	88.6 ± 0.4	47.8 ± 0.5	37.0 ± 0.3	69.56	52.37	17.19	0.973
	PU-BDO	99.0 ± 0.6	88.9 ± 0.3	45.0 ± 0.5	40.0 ± 0.6	70.02	51.33	18.70	0.979
	PU-DPG	100.1 ± 0.5	88.7 ± 0.3	46.5 ± 0.4	39.3 ± 0.3	71.27	50.63	20.64	0.988
480 h	PU-PURE	104.7 ± 0.9	86.9 ± 0.6	36.5 ± 0.5	30.1 ± 0.4	71.79	55.86	15.93	0.998
	PU-MEG	100.5 ± 0.5	84.0 ± 0.3	40.0 ± 0.2	32.7 ± 0.5	72.95	54.55	18.40	0.987
	PU-BDO	96.2 ± 0.4	84.9 ± 0.3	43.5 ± 0.4	37.0 ± 0.5	72.98	52.30	20.68	0.976
	PU-DPG	97.5 ± 0.7	85.2 ± 0.4	41.0 ± 0.2	36.2 ± 0.3	74.38	52.14	22.24	0.991
960 h	PU-PURE	101.5 ± 0.2	86.7 ± 0.5	17.5 ± 0.8	27.3 ± 0.6	75.18	57.67	17.51	0.998
	PU-MEG	100.2 ± 0.3	85.0 ± 0.2	28.5 ± 0.7	30.5 ± 0.9	74.37	56.08	18.29	0.998
	PU-BDO	93.6 ± 0.8	82.0 ± 0.3	35.2 ± 0.5	36.8 ± 0.2	76.09	52.83	23.26	0.988
	PU-DPG	95.2 ± 0.9	83.7 ± 0.4	33.0 ± 0.6	33.8 ± 0.7	77.15	53.49	23.67	0.994

Table S2. Polymer density in diferentes hydrolysis time

	Sample	ρ_P (g.cm ⁻³)
0h	PU-PURE	1.0712 ± 0.0102
	PU-MEG	1.0779 ± 0.0101
	PU-BDO	1.0495 ± 0.0034
	PU-DPG	1.0156 ± 0.0008
480h	PU-PURE	1.0623 ± 0.0013
	PU-MEG	1.1120 ± 0.0065
	PU-BDO	1.1118 ± 0.0034
	PU-DPG	1.0156 ± 0.0025
960h	PU-PURE	1.0558 ± 0.0047
	PU-MEG	1.0805 ± 0.0049
	PU-BDO	1.1554 ± 0.0041
	PU-DPG	1.0843 ± 0.0019

**Figure S1.** Storage modulus, E' as function of temperature for samples without hydrolysis

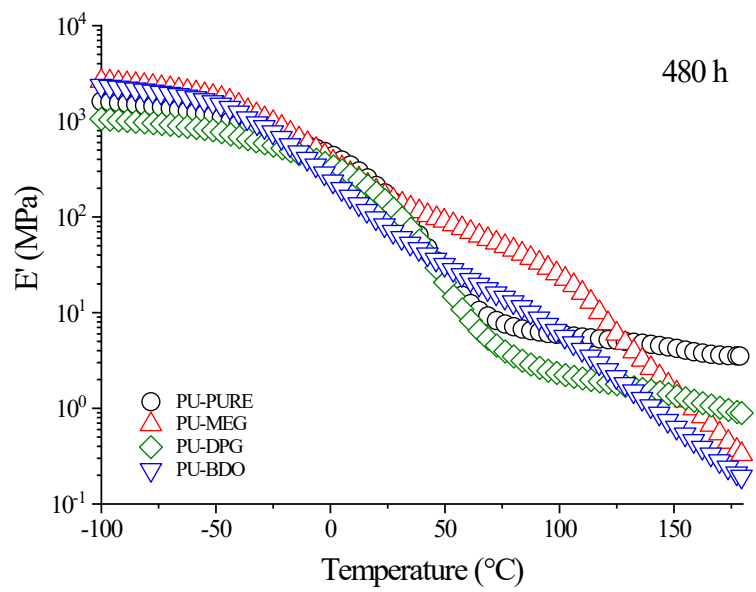


Figure S2. Storage modulus, E' as function of temperature for samples hydrolyzed 480h

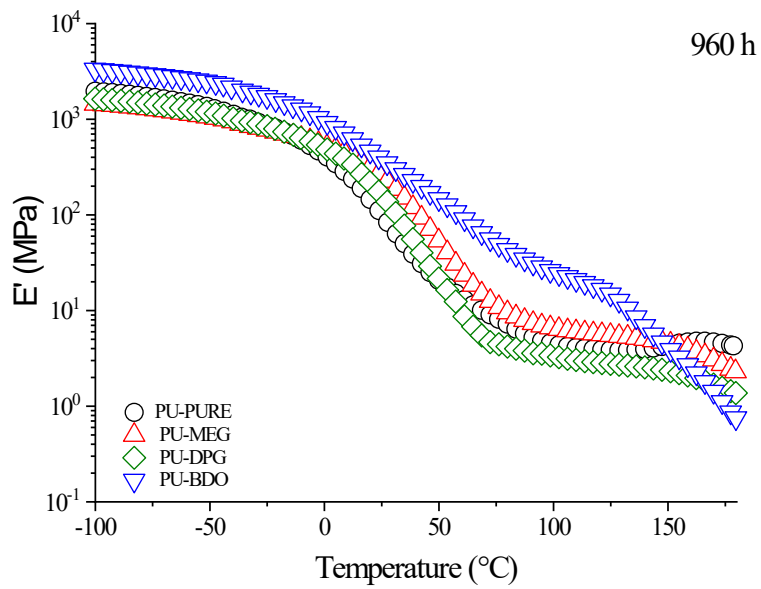
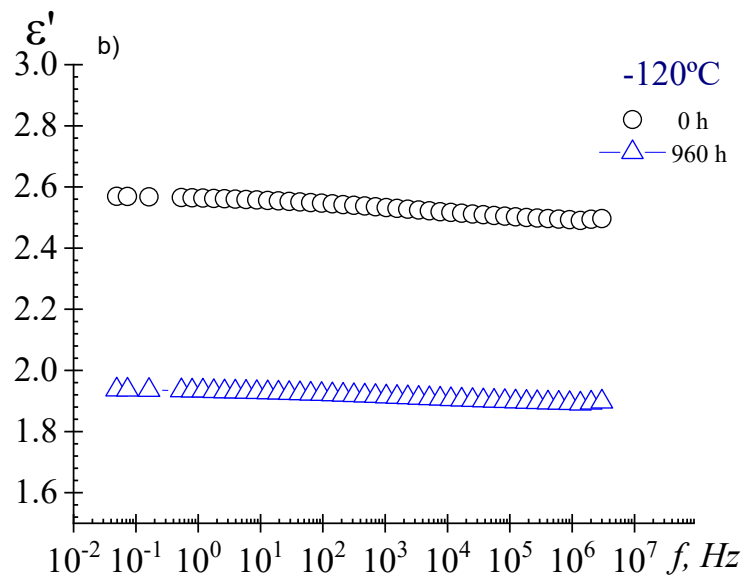
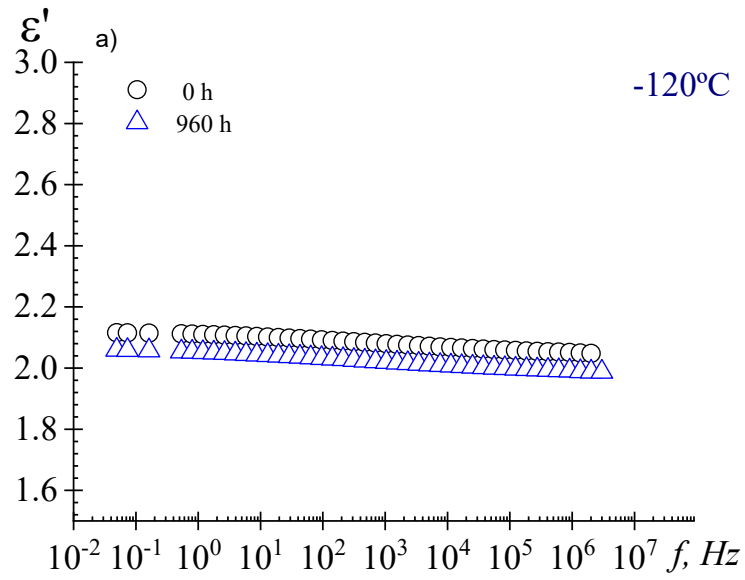


Figure S3. Storage modulus, E' as function of temperature for samples hydrolyzed 960h



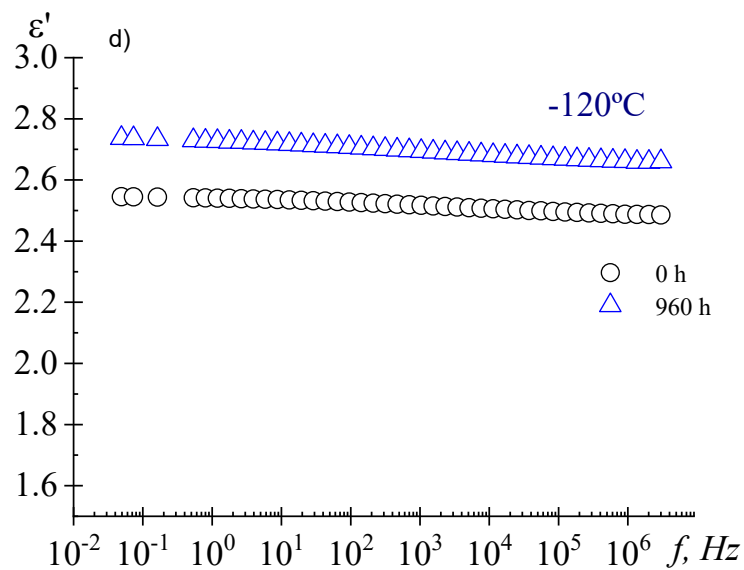
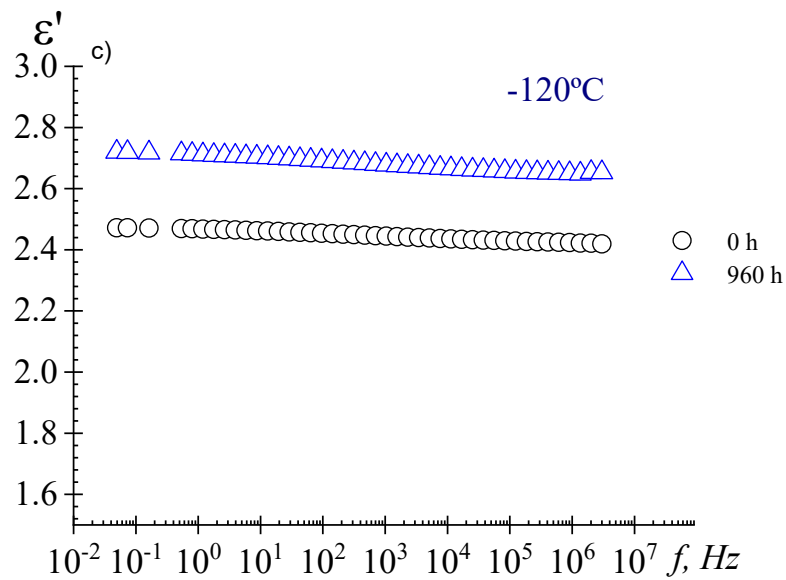


Figure S4. Frequency dependence of dielectric constant (ϵ') in the γ -transition of a) PU-PURE, b) PU-MEG, c) PU-DPG and d) PU-BDO

1 Daniel K Owens, and RC Wendt, 'Estimation of the Surface Free Energy of Polymers', Journal of applied polymer science, 13 (1969), 1741-47.